

Synthesis, single crystal X-ray structure determination and NMR studies of $\text{Cp}_2\text{Fe}(\text{PPh}_2)_2\text{PtPh}_2$ and $\text{Cp}_2\text{Fe}(\text{PPh}_2)_2\text{PtI}_2$

Thomas J. Colacot ^{a,*}, Richard A. Teichman ^a, Raymundo Cea-Olivares ^b,
J-Guadalupe Alvarado-Rodríguez ^b, Rubén A. Toscano ^b, Walter J. Boyko ^c

^a Organometallic Chemicals & Catalysts Development, Precious Metals Division, Johnson Matthey, 2001 Nolte Drive, West Deptford, NJ 08066, USA

^b Instituto de Química, Universidad Nacional Autónoma México Circuito Exterior, Ciudad Universitaria, México, 04510 D.F, Mexico

^c Department of Chemistry, Villanova University, Villanova, PA 19085, USA

Received 24 June 1997

Abstract

Diphenyl[1,1'-bis(diphenylphosphino)ferrocene]platinum(II), $\text{Cp}_2\text{Fe}(\text{PPh}_2)_2\text{PtPh}_2$ (**1**) and diiodo[1,1'-bis(diphenylphosphino)ferrocene]platinum(II), $\text{Cp}_2\text{Fe}(\text{PPh}_2)_2\text{PtI}_2$ (**2**) were synthesized in nearly quantitative yield, with excellent purity by allowing $\text{Cp}_2\text{Fe}(\text{PPh}_2)_2$ to react with (COD)PtPh₂ and (COD)PtI₂ (COD = 1,5-cyclooctadiene), respectively. Compounds **1** and **2** have been well characterized by various analytical and spectroscopic techniques and also by single crystal X-ray diffraction. Platinum in both the complexes seemed to have a distorted square planar geometry. Interestingly, the respective bite angles (P–Pt–P bond angle) in **1** (101.2(1) Å) and **2** (100.6(1) Å) deviate from the ideal 90° situation and are larger than in the reported structure, dppfPtCl₂ [dppf = 1,1'-bis(diphenylphosphino)ferrocene]. A detailed NMR study, including 2D and simulation experiments has been performed on these compounds for complete structural assignment. The compounds **1** and **2** crystallized in triclinic space groups P $\bar{1}$ and P $\bar{1}$ with $a = 12.268(2)$ Å, 10.089 (1); $b = 13.043(2)$ Å, 10.856 (1); $c = 13.649(1)$, 17.787(1) Å; $\alpha = 100.49(1)$, 86.75(1)°; $\beta = 93.12(1)$, 77.52(1)°; $\gamma = 103.44(1)$, 64.91(1)°; $V = 2078.0(5)$, 1721.3(3) Å³ and $Z = 2$ and 2, respectively. The final refinements of **1** and **2** converged at $R = 0.0388$ and 0.0580, respectively. © 1998 Elsevier Science S.A. All rights reserved.

Keywords: Platinum diphosphine complexes; Homogeneous catalysts; NMR; X-ray diffraction; Triclinic

1. Introduction

Because of their large bite angles, longer metal-phosphorus bonds, and *cis* phosphine configuration, 1,1'-bis(diphenylphosphino)ferrocene (dppf) complexes of precious metal groups act as far superior catalysts [1] in homogenous catalysis, especially in Grignard cross coupling reactions [2], hydrogenation reactions [3], regioselective synthesis [4], olefin reduction [5], olefin hydroformylation [6], stereospecific nucleophilic substitution [7], carbonylation and carbonylative coupling [8], and also in polymerization and poly condensation reactions [9], in comparison to the complexes of conven-

tional monodentate or bidentate phosphines [1]. Among the large variety of metal-dppf complexes, dppfPdCl₂ is one of the most widely studied systems. The synthesis and X-ray structure of dppfPdCl₂ was reported thrice in the literature by three independent groups of workers ([2]a[3]b[10]) during the period 1984–1995, showing its structural and theoretical importance. However, the synthesis and the crystal structure of the analogous Pt compound, dppfPtCl₂ was reported [10] only in 1995 by Filgueiras et. al. A variable temperature NMR report is also available [11] on the fluxional behavior of the Cp-protons in dppfPt(CH₂SiMe₂CH=CH₂)₂. Apart from their applications in homogeneous catalysis, recently Stang et.al, has explored the geometry of dppfMCl₂ (M = Pt and Pd) in supramolecular chem-

* Corresponding author. e-mail: colactj@matthey.com

istry, to prepare reactive Pt(II) and Pd(II) complexes, suitable for the self-assembly of macromolecular squares [12].

To our knowledge, so far no other similar examples of dppf complexes of Pt and Pd compounds are reported in the literature. Since the catalytic efficacy of a complex is greatly influenced by the steric and elec-

tronic environment around the metal ion, M–X bond lability (X is a group other than dppf) and the overall geometry of the complex, we decided to focus our attention on the synthesis of novel derivatives of these types of compounds with a long term objective to study their applications in homogeneous catalysis for organic transformations. These types of complexes and their study may serve as a prelude to our recent projects on precious metal catalysts containing chiral biphosphines. We are also exploring the synthesis and potential applications of Pt, Pd and Ni based dppf complexes for Ziegler–Natta catalysis in analogy with Brookhart's Pd and Ni complexes of macrocyclic amines [13], and the recently reported cationic Pt(II) system, (Bu₂bpy)MePt⁺ by Puddephatt [14]. Herein, we report our preliminary results in this area on the synthesis, X-ray structures and NMR studies of two novel Pt compounds, one where there is a labile substituent, iodo- on the Platinum, Cp₂Fe(PPh₂)₂PtI₂ (Fig. 2) and the latter where the Pt is bonded to an aryl group, Cp₂Fe(PPh₂)₂PtPh₂ (Fig. 1).

Table 1
Crystallographic data^a for **1**^b and **2**^b

	1	2
Molecular formula	C ₄₇ H ₄₀ Cl ₂ FeP ₂ Pt	C _{34.35} H _{28.7} Cl _{0.7} FeI ₂ P ₂ Pt
<i>F</i> _w	988.6	1033.0
Crystal system	Triclinic	Triclinic
Space group	P1	P1
Unit cell dimension		
<i>a</i> (Å)	12.268 (2)	10.089 (1)
<i>b</i> (Å)	130.43 (2)	10.856 (1)
<i>c</i> (Å)	13.648 (1)	17.787 (1)
<i>α</i> (°)	100.49 (1)	86.75 (1)
<i>β</i> (°)	93.12 (1)	77.52 (1)
<i>γ</i> (°)	103.44 (1)	64.91 (1)
<i>V</i> (Å ³)	2078.0 (5)	1721.3 (3)
<i>Z</i>	2	2
<i>D</i> _{calc}	1.580	1.993
<i>F</i> (000)	980.00	973.40
Absorption coefficient (mm ⁻¹)	3.949	6.444
Crystal dimension (mm)	0.76 × 0.60 × 0.56	0.44 × 0.28 × 0.14
Scan type	<i>ω</i>	<i>ω</i>
Scan speed in <i>ω</i>	4.0, 60.0	4.0, 60.0
Deg min ⁻¹ , min, max } 2 <i>θ</i> range, deg	3.0, 60.0	3.0, 60.0
Temperature (K)	293	
Index ranges	0 ≤ <i>h</i> ≤ 17, -17 ≤ <i>k</i> ≤ 17, -19 ≤ <i>l</i> ≤ 19	0 ≤ <i>h</i> ≤ 14, -13 ≤ <i>k</i> ≤ 15, -24 ≤ <i>l</i> ≤ 25
Data collected	12574	10569
No. of obsd rfln, } <i>F</i> > 4.0σ(<i>F</i>)	9593	5026
No. of params refined	497	398
GOF	1.03	1.24
<i>R</i> ^c	0.0388	0.0584
<i>R</i> _w	0.0413	0.0697
Largest and mean Δ/σ	0.004, 0.001	0.290, 0.010
Largest difference peak	1.42 eÅ ⁻³	2.80 eÅ ⁻³
Largest difference hole	-1.29 eÅ ⁻³	-2.49 eÅ ⁻³
Weig sch. (w ⁻¹)	σ ² (<i>F</i> _o) + 0.0004 <i>F</i> _o ²	σ ² (<i>F</i> _o) + 0.0008 <i>F</i> _o ²
Min/max transmission	0.2350/0.5300	0.1335/0.9352

^a Graphite-monochromatized Mo-K_α radiation, λ = 0.71073 Å.

^b Both compounds **1** and **2** contain 1 and 1/3 of CH₂Cl₂ molecule respectively in the crystal lattices.

^c $R = \frac{\sum \|F_o\| - |F_c|}{\sum |F_o|}$; $R_w = \frac{[\sum (w(F_o^2 - F_c^2))] / [\sum (w(F_o^2))]^{1/2}}{S}$; $S = [\sum (w|F_o - F_c|^2) / (\text{no. relns} - \text{no. params})]^{1/2}$.

2. Experimental

2.1. General procedures

All the reactions and subsequent manipulations were performed under a N₂ atmosphere using standard Schlenk line techniques in conjunction with a glove box (Vacuum Atmospheres Model HE-493/MO-5). The starting materials, Cp₂Fe(PPh₂)₂, (COD)PtI₂ and (COD)PtPh₂ were either prepared in the development laboratory or obtained as samples from the production facility. These materials were freshly recrystallized and their purities were checked by ¹H-, ¹³C- and ³¹P-NMR spectroscopy prior to the reactions. All the solvents were either purchased from Johnson Matthey catalog company, Alfa–Aesar or Aldrich Chemicals and purified using standard procedures [15].

Proton, ¹³C- and ³¹P-NMR spectral data were collected on a Varian XL-300 FT NMR spectrometer operating at 300.1, 75.5 and 121.1 MHz, respectively, as CDCl₃ or CD₂Cl₂ solution. The ¹H and ¹³C shifts were referenced to TMS in the solvent, while the ³¹P chemical shifts were referenced to an external standard, 85% H₃PO₄. Two-dimensional carbon–hydrogen correlation NMR (HETCOR 2D) were recorded with a standard Varian pulse sequence. Spin simulation of the spectra were performed on a MS-DOS PC using NUTS, a NMR data processing from Acorn NMR. All the platinum coupling constants are reported as absolute values. FT-IR spectra were obtained on a Nicolet 750 spectrophotometer using KBr pellets. Elemental analysis were done at E + R Microanalytical laboratory, Corona, NY. Melting points were determined on a

Table 2
Atomic coordinates and anisotropic displacement coefficients ($\text{\AA}^2 \times 10^3$) for dppfPtPh_2

Atom	x	y	z	U_{eq}	
Pt	2108(1)	2345(1)	7411(1)	27(1)	
Fe	4498 (1)	5310(1)	7169(1)	34(1)	
P(1)	4048(1)	2702(1)	7416(1)	29(1)	
P(2)	1790(1)	3994(1)	7277(1)	29(1)	
C(1)	395(4)	1792(3)	7351(4)	35(1)	
C(2)	–253(5)	1310(4)	6445(5)	48(2)	
C(3)	–1422(5)	944(4)	6393(6)	59(2)	
C(4)	–1979(5)	1044(5)	7240(7)	66(3)	
C(5)	–1355(5)	1488(5)	8151(6)	62(2)	
C(6)	–187(5)	1853(5)	8211(5)	47(2)	
C(7)	2093(4)	823(4)	7614(5)	42(2)	
C(8)	2074(5)	596(5)	8579(6)	57(2)	
C(9)	2068(7)	–442(4)	8734(8)	86(4)	
C(10)	2073(8)	–1245(7)	7943(11)	107(6)	
C(11)	2055(8)	–1065(6)	6985(10)	99(5)	
C(12)	2060(6)	–28(4)	6830(6)	62(3)	
C(13)	4446(4)	2138(4)	6203(4)	34(1)	
C(14)	5523(5)	1977(4)	6094(5)	46(2)	
C(15)	5777(6)	1509(5)	5172(5)	60(3)	
C(16)	4991(7)	1206(5)	4366(5)	65(3)	
C(17)	3938(7)	1375(4)	4451(5)	60(2)	
C(18)	3659(5)	1833(4)	5371(4)	45(2)	
C(19)	4780(4)	2093(4)	8272(4)	37(2)	
C(20)	5333(6)	2681(5)	9172(5)	64(3)	
C(21)	5839(8)	2169(8)	9816(7)	91(4)	
C(22)	5821(6)	1113(8)	9573(7)	82(4)	
C(23)	5281(6)	525(6)	8662(7)	67(3)	
C(24)	4757(5)	1015(5)	8024(5)	52(2)	
C(25)	509(4)	3915(4)	6482(4)	67(3)	
C(26)	527(5)	3753(5)	5466(5)	56(2)	
C(27)	–456(7)	3619(6)	4840(7)	80(3)	
C(28)	–1433(6)	3671(6)	5241(8)	84(4)	
C(29)	–1469(5)	3834(7)	6245(9)	88(4)	
C(30)	–499(5)	3952(5)	6891(6)	62(3)	
C(31)	1623(4)	4746(4)	8492(4)	38(2)	
C(32)	1201(5)	5664(4)	8597(5)	52(2)	
C(33)	1144(6)	6251(5)	9538(6)	67(3)	
C(34)	1495(7)	5918(6)	10385(6)	75(3)	
C(35)	1897(7)	5026(6)	10292(5)	67(3)	
C(36)	1958(5)	4426(4)	9350(4)	46(2)	
C(37)	2817(4)	4970(3)	6799(4)	32(1)	
C(38)	3390(4)	4757(4)	5922(4)	40(2)	
C(39)	4156(5)	5738(5)	5835(5)	53(2)	
C(40)	4050(5)	6542(4)	6628(5)	51(2)	
C(41)	3237(4)	6086(4)	7222(4)	41(2)	
C(42)	4902(4)	4065(4)	7678(4)	33(1)	
C(43)	5772(4)	4539(4)	7127(5)	43(2)	
C(44)	6190(4)	5649(5)	7593(6)	56(2)	
C(45)	5617(5)	5855(4)	8437(5)	55(2)	
C(46)	4807(5)	4899(4)	8498(4)	42(2)	
C(47)	921(10)	1218(8)	2247(11)	124(7)	
C1(1A)	1368(5)	2150(4)	3313(4)	167(3)	sof = 0.80
C1(1B)	863(14)	2510(17)	2042(43)	310(29)	sof = 0.20
C1(2A)	2125(12)	1363(7)	1512(8)	212(7)	sof = 0.50
C1(2B)	1067(10)	1654(14)	1150(8)	232(10)	sof = 0.50

* Equivalent isotropic U defined as one third of the trace of the orthogonalized U_{ij} tensor.

Thomas–Hoover melting point apparatus using sealed capillaries and are uncorrected.

2.2. Synthesis of $Cp_2Fe(PPh_2)_2PtPh_2$

To a 250 ml side arm Schlenk flask containing a stirred solution of 1,1'-bis(diphenylphosphino)ferrocene, dppf (5.60 g, 10.1 mmol) in methylene chloride (100 ml), (COD)PtPh₂ (4.57 g, 10.0 mmol) was

Table 3
Atomic coordinates and anisotropic displacement coefficients ($\text{\AA} \times 10^3$) for dppfPtI₂

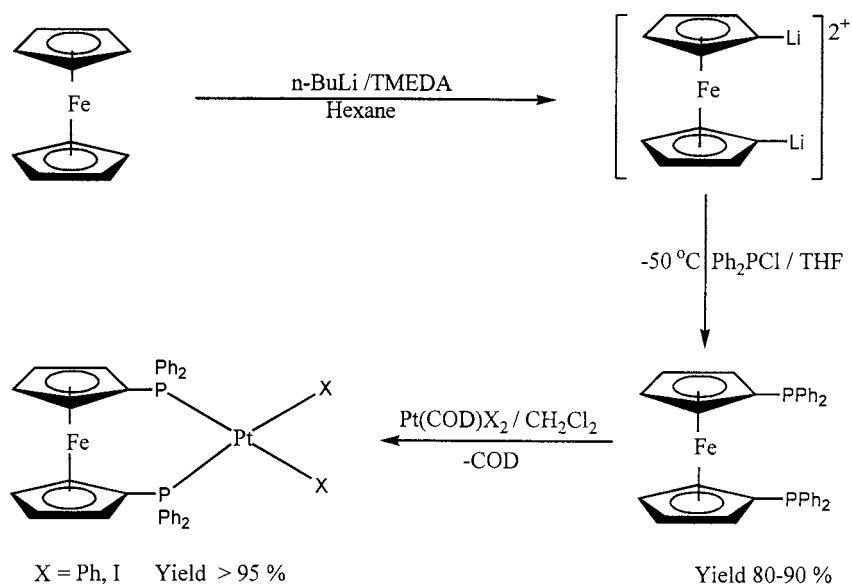
Atom	x	y	z	U(eq)
Pt	3406(1)	4267(1)	2278(1)	27(1)
I(1)	1430(2)	6014(1)	1527(1)	77(1)
I(2)	2626(2)	6341(1)	3255(1)	55(1)
Fe	7147(3)	380(2)	1871(1)	32(1)
P(1)	4793(5)	3009(3)	3134(2)	30(1)
P(2)	3984(5)	2624(3)	1361(2)	29(1)
C(1)	3653(20)	2819(16)	4035(9)	41(6)
C(2)	2098(22)	3463(17)	4188(9)	46(7)
C(3)	1262(25)	3241(19)	4868(11)	58(8)
C(4)	1942(29)	2429(22)	5412(12)	66(11)
C(5)	3453(29)	1807(23)	5284(11)	78(11)
C(6)	4322(23)	1954(19)	4583(10)	58(8)
C(7)	6031(20)	3707(15)	3360(10)	42(6)
C(8)	6162(29)	3921(29)	4098(12)	82(14)
C(9)	7108(30)	4412(30)	4241(14)	91(15)
C(10)	8028(26)	4671(25)	3633(15)	76(11)
C(11)	8005(28)	4394(24)	2862(14)	70(12)
C(12)	6985(29)	3936(22)	2755(12)	66(12)
C(13)	2996(17)	1574(14)	1651(9)	33(5)
C(14)	2035(25)	1769(23)	2335(11)	60(10)
C(15)	1317(35)	960(30)	2592(16)	93(17)
C(16)	1585(31)	-102(30)	2119(20)	95(17)
C(17)	2441(28)	-348(22)	1404(18)	79(13)
C(18)	3134(22)	535(16)	1156(13)	57(8)
C(19)	3621(20)	3158(14)	415(8)	37(6)
C(20)	2292(26)	3322(19)	211(12)	57(10)
C(21)	2048(30)	3691(18)	-527(13)	72(11)
C(22)	3067(41)	3903(27)	-1048(14)	101(19)
C(23)	4438(34)	3724(24)	-889(12)	76(13)
C(24)	4677(25)	3405(21)	-159(11)	63(10)
C(25)	6066(16)	1222(13)	2927(7)	29(5)
C(26)	7650(19)	650(15)	2879(8)	37(6)
C(27)	8171(20)	-788(16)	2723(9)	43(6)
C(28)	7027(21)	-1073(15)	2637(8)	39(6)
C(29)	5638(19)	152(15)	2793(9)	38(6)
C(30)	5960(17)	1460(14)	1109(7)	29(5)
C(31)	7135(19)	1862(18)	1100(9)	41(6)
C(32)	8525(22)	681(22)	902(9)	58(8)
C(33)	8235(20)	-460(18)	760(9)	50(7)
C(34)	6651(20)	24(14)	892(8)	39(6)
C1(1)	2492(34)	-457(23)	4232(16)	123(15)
C1(2a)	-802(47)	1152(46)	4578(20)	92(23)
C1(2b)	-708(62)	249(60)	4379(16)	93(32)
C(35)	738(64)	-488(46)	4870(53)	73(34)

* Equivalent isotropic U defined as one third of the trace of the orthogonalized U_{ij} tensor.

Table 4
Selected bond distances and angles of complex 1 and 2

Bond distances (\AA)		Bond angles ($^\circ$)	
Complex 1			
Pt–P(1)	2.316(1)	P(1)–Pt–P(2)	101.2(1)
Pt–P(2)	2.310(1)	P(1)–Pt–C(7)	89.1(1)
Pt–C(1)	2.049(4)	P(2)–Pt–C(1)	87.0(2)
Pt–C(7)	2.050(6)	C(1)–Pt–C(7)	82.9(2)
P(1)–C(13)	1.825(5)	Pt–P(1)–C(13)	111.0(2)
P(1)–C(19)	1.833(6)	Pt–P(1)–C(19)	116.1(2)
P(1)–C(13)	1.802(4)	Pt–P(1)–C(42)	121.0(2)
P(2)–C(25)	1.831(5)	Pt–P(2)–C(25)	114.4(2)
P(2)–C(31)	1.815(5)	Pt–P(2)–C(31)	110.9(2)
P(2)–C(37)	1.811(5)	Pt–P(2)–C(37)	120.9(2)
Fe–C(37–41) av.	2.037	C(13)–P(1)–C(42)	103.1(2)
Fe–C(41–46) av.	2.039	C(13)–P(1)–C(19)	102.1(2)
		C(25)–P(2)–C(37)	102.4(2)
		C(25)–P(2)–C(31)	105.2(2)
Complex 2			
Pt–P(1)	2.281(4)	P(1)–Pt–P(2)	100.6(1)
Pt–P(2)	2.285(4)	P(1)–Pt–I(2)	84.4(1)
Pt–I(1)	2.648(2)	P(2)–Pt–I(1)	89.0(1)
Pt–I(2)	2.657(1)	I(1)–Pt–C(1)	86.1(1)
P(1)–C(1)	1.816(17)	Pt–P(1)–C(1)	113.0(6)
P(1)–C(7)	1.831(13)	Pt–P(1)–C(7)	112.8(5)
P(1)–C(25)	1.820(12)	Pt–P(1)–C(25)	121.4(5)
P(1)–C(13)	1.799(19)	Pt–P(2)–C(13)	112.2(5)
P(2)–C(19)	1.811(15)	Pt–P(2)–C(19)	118.2(5)
P(2)–C(30)	1.820(14)	Pt–P(2)–C(30)	114.6(6)
Fe–C(25–29) av.	2.047	C(1)–P(1)–C(7)	108.1(9)
Fe–C(25–29) av.	2.044	C(7)–P(1)–C(25)	101.7(7)
		C(13)–P(2)–C(19)	103.9(9)
		C(19)–P(2)–C(30)	100.6(6)

added all at once and stirred for another 30 min. No noticeable color change was observed during this period. The mixture was then refluxed overnight to obtain a yellow solution with some precipitate. The reaction mixture was then allowed to cool to RT, concentrated to 10–20 ml under vacuum, followed by the addition of Et₂O (100 ml) to precipitate out the compound. The yellow solid was then filtered using a Schlenk glass frit, the solid was washed twice with 20 ml of Et₂O, and dried under vacuum to obtain a pale yellow crystalline compound, **1** (9.6 g, 9.7 mmol, 97% yield). This was further recrystallized using CH₂Cl₂/toluene mixture at –15°C to obtain transparent pale yellow crystals (M.p. 192°C dec.) of dppfPtPh₂.CH₂Cl₂. Anal. Calcd for C₄₇H₄₂FeP₂PtCl₂: C, 56.98; H, 4.27; Fe, 5.64; Pt, 19.69. Found: C, 56.99; H, 4.45; Fe, 5.35; Pt, 19.96. IR(cm⁻¹): 3140 (vw) 3109 (vw), 3082 (vw), 3048 (s), 2996 (m), 2969 (w), 1568 (s), 1478 (s), 1433 (s), 1385 (w), 1308 (m), 1264 (w), 1196 (m), 1165 (s), 1096 (s), 1064 (m), 1029 (s), 996 (m), 967 (w), 886 (w), 842 (w), 818 (m), 731 (vs), 697 (vs), 640 (m), 591 (vw), 546 (s), 519 (s), 494(vs), 465 (s), 435 (s)

Scheme 1. Synthesis of dppf PtPh_2 , dppf PtI_2 from ferrocene.

2.3. Synthesis of $\text{Cp}_2\text{Fe}(\text{PPh}_2)_2\text{PtI}_2$

$\text{Pt}(\text{COD})\text{I}_2$ (5.57 g, 10.0 mmol) was added to a stirred solution of dppf (5.54 g, 10.0 mmol) in CH_2Cl_2 (100 ml) as described above. A clear solution resulted within minutes, which on further stirring for an hour started to give a yellow precipitate. The stirring was continued overnight at room temperature. The solution was then concentrated to 1/5 th of its original volume, and mixed with Et_2O (100 ml). The resulted yellow solid was filtered, washed with Et_2O (20 ml \times 2) and then dried under vacuum to obtain an analytically pure sample of $\text{dppfPtI}_2 \cdot 1/3\text{CH}_2\text{Cl}_2$ (9.9 g, 9.6 mmol, 96% yield, M.p. 320°C dec.). Anal. Calcd for $\text{C}_{34.33}\text{H}_{30.66}\text{FeP}_2\text{PtI}_2\text{C}_{10.66}$: C, 39.90; H, 2.99; Cl, 2.27; I, 24.56. Found: C, 39.89; H, 2.94; Cl, 2.55; I, 25.27. IR(cm^{-1}): 3081 (w), 3056 (w), 1660 (vw), 1596 (vw), 1592 (vw), 1588 (vw), 1529 (vw), 1481 (w), 1436 (s), 1387 (vw), 1308 (w), 1263 (vw), 1191 (w, sh), 1169 (w), 1096 (s), 1034 (w), 1002 (vw), 846 (vw), 824 (vw), 745 (m), 694 (vs), 639 (w), 658 (s), 495 (vs), 469 (s), 442 (w).

2.4. X-Ray structural analysis

Pale yellow crystals of **1** were grown by diffusing toluene into a concentrated solution of dppfPtPh_2 in dry CH_2Cl_2 at low temperature (-15°C), while single crystals of **2** were obtained by slow evaporation of a solution of CH_2Cl_2 /hexane in an NMR tube. The crystals were coated with an epoxy resin and mounted on a Siemens P4/PC diffractometer using highly oriented graphite-monochromated Mo- K_α ($\lambda = 71073 \text{ \AA}$) radiation. The final unit cell parameters summarized in Table 1, were obtained by a least squares fit of 39

accurately centered reflections in the ranges, $9^\circ \leq 2\theta \leq 25^\circ$ and the intensity data were collected at 293 K in the ranges $3^\circ \leq 2\theta \leq 60^\circ$, using ω scan technique. Three standard reflections measured after every 97 reflections did not show any significant change in intensity during data collection for **1**. A linear decay (10.5%) correction was applied for **2** based on standards, and there was no significant variation in the intensities of these standards. Both sets of data were corrected for Lp and absorption effects (Ψ -scans). The structures were solved by direct methods [16] and refined by full matrix least squares using anisotropic thermal parameters for all non-hydrogen atoms. All the hydrogen atoms were included as fixed contributions and are not refined. Their idealized positions were generated from the geometries about the attached carbon atoms, and forced to ride on it with a fixed isotropic temperature factor, $U = 0.08 \text{ \AA}^2$ and C–H distances of 0.96 \AA . The structures were refined by using SHELXTL-PLUS PC version [17]. The quantity minimized during the least squares analysis was $\Sigma = w|F_o - F_c|^2$ where $w^{-1} = \sigma(|F_o|) + 0.0008(|F_o|)^2$. The final cycles of refinement of the structures including disordered solvent molecules are listed in Table 1, while the anisotropic temperature factors are listed in Tables 2 and 3. The selected bond lengths and bond angles of **1** and **2** are listed in Table 4.

3. Results and discussion

As given in Scheme 1, both $\text{Cp}_2\text{Fe}(\text{PPh}_2)_2\text{PtPh}_2$ and $\text{Cp}_2\text{Fe}(\text{PPh}_2)_2\text{PtI}_2$ have been synthesized in high yield with excellent purity by allowing $\text{Pt}(\text{COD})\text{Ph}_2$ and Pt -

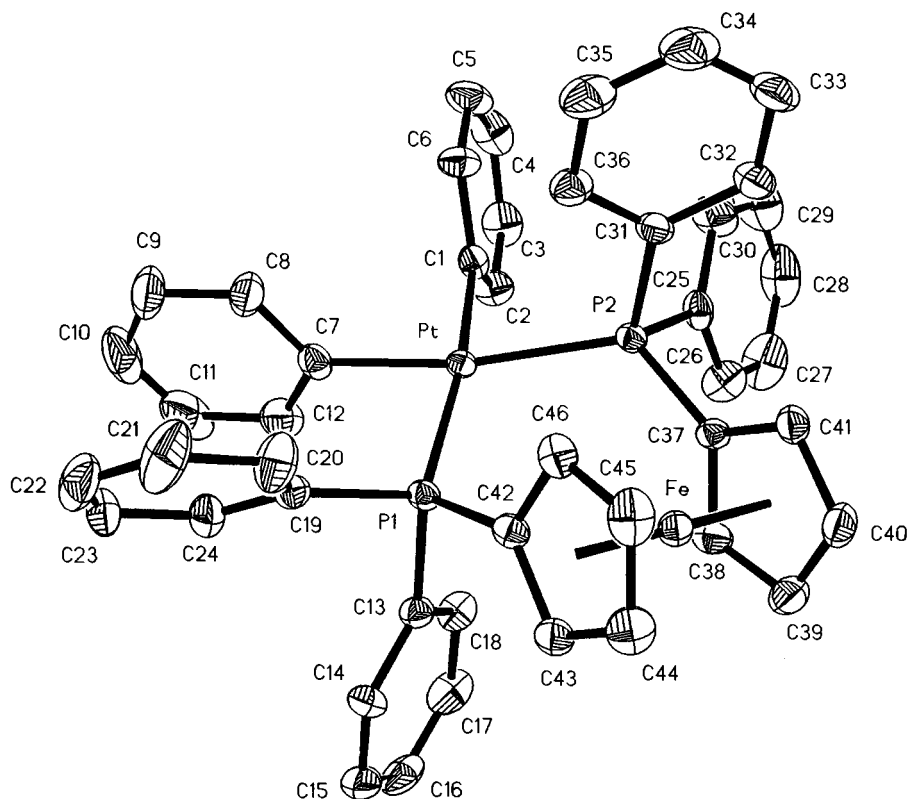


Fig. 1. ORTEP diagram of $\text{Cp}_2\text{Fe}(\text{PPh}_2)_2\text{PtPPh}_2$, showing 30% probability ellipsoids.

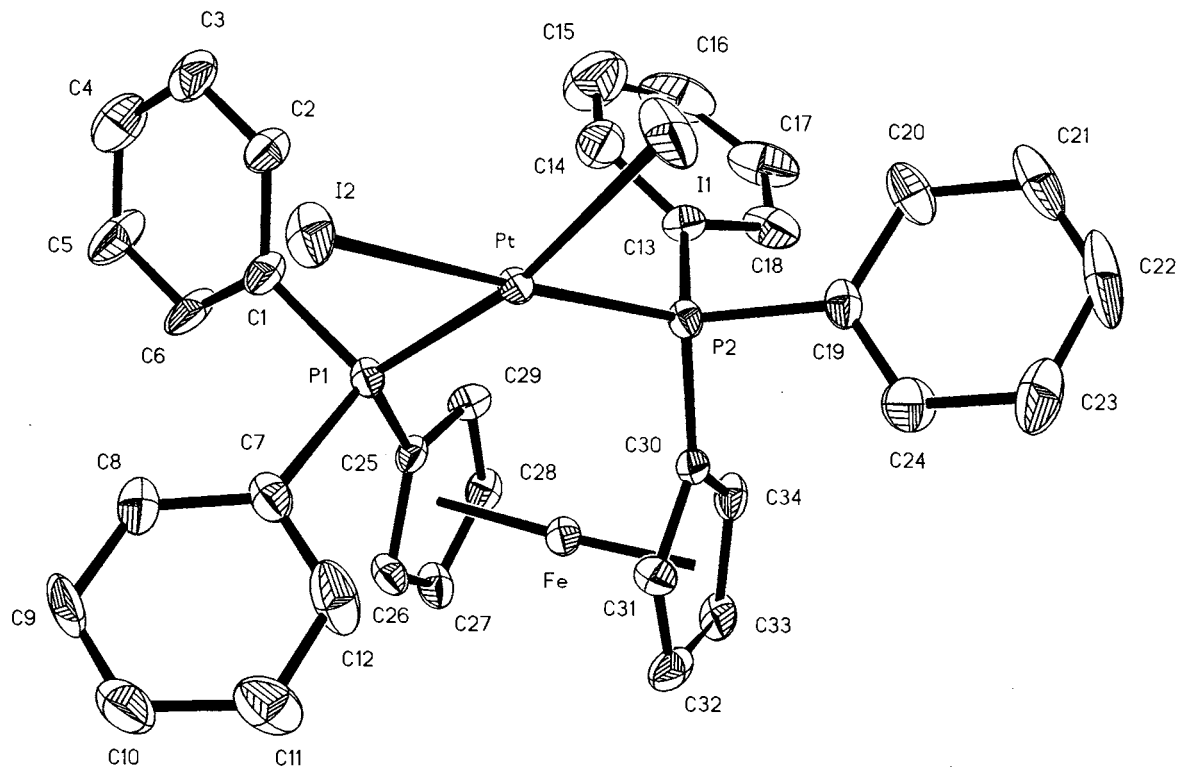


Fig. 2. ORTEP diagram of $\text{Cp}_2\text{Fe}(\text{PPh}_2)_2\text{PtI}_2$, showing 30% probability ellipsoids.

Table 5

¹H-NMR spectral data of dppf, dppfPtI₂ and dppfPtPh₂ in CDCl₃

Atom numbering	dppf δ (ppm)	dppfPtI ₂ δ (ppm)	dppfPtPh ₂ δ (ppm)
H2	3.99, q (1.88 Hz) ^a	4.16, q (1.9 Hz) ^a	4.30, q (1.8 Hz) ^a
H3	4.24, t	4.31, cm	4.21, t
H5	b	7.90, cm	7.49, cm
H6	b	7.38, cm	7.25, cm
H7	b	7.45, cm	7.34, cm
H9	—	—	6.87, cm (² J _{Pt-H9} = 57.9 Hz)
H10	—	—	6.43, cm
H11	—	—	6.35, cm

Shifts in ppm relative to TMS.

q, quintet; t, triplet; cm, complex multiplet.

^a Separation between major lines in multiplet.^b These shifts form a tight complex multiplet covering 7.26–7.36 ppm.

(COD)I₂ to react with 1,1'-bis(diphenylphosphino)ferrocene, dppf in CH₂Cl₂ solvent. Unlike the synthesis ([18,3]b) of the orange red colored Cp₂Fe(PPh₂)₂PdCl₂, it has been fairly difficult to monitor the reaction involving the formation of **1** visually, as the reactants do not seem to go in to solution completely with the concomitant formation of the yellow product. However, in the case of **2**, a clear solution resulted, upon mixing the reactants, followed by the formation of a yellow precipitate formation.

Both compounds are soluble in chlorinated solvents such as CH₂Cl₂ and CHCl₃ and insoluble or sparingly soluble in hydrocarbon solvents and ether as in the case of Cp₂Fe(PPh₂)₂MCl₂ (M = Pt or Pd) ([2]a[3]b[10]). The melting point of **2** is very high (320°C dec.) in comparison to that of **1** (192°C). This could be due the ionic nature of the Pt–I bond. Both compounds **1** and **2** are reasonably stable to air and moisture. However samples kept in a vial at room temperature changed to yellowish brown within weeks unlike the samples stored in cold under N₂.

Complex **1** crystallizes very readily in a mixture of hydrocarbon and CH₂Cl₂ solvent to give shining transparent crystals, which become opaque and powdery on drying due to the loss of solvent from the lattice. Although **2** can be recrystallized in a similar way, it was very difficult to obtain single crystals by this method. X-ray quality crystals have been obtained only by a careful slow evaporation of the solvent in a narrow tube (eg. NMR tube). The crystals, especially of **2**, when not in contact with the solvent become flaky and non diffracting. This posed further problem in solving the structure and we had to make a dozen attempts to get publishable quality structure.

Elemental analyses of **1** and **2** have indicated that these compounds contain 1 and 1/3 molecules of the solvent, CH₂Cl₂, respectively, in the lattice. While we were puzzled by the elemental analysis data of **2**, as it is not very common to have a molecule with 1/3 molecule of solvent in the lattice, an independent X-ray analysis

precisely came up with the proposed structure. These compounds on grinding followed by drying, or on long standing for a few days at room temperature gave analyses correspond to **1** and **2** having no solvent of crystallization.

As expected, in both **1** and **2** the Fe atom is sandwiched between two staggered Cp rings. The two distorted tetrahedral phosphine moieties are bonded to a Pt atom, which is in a distorted square planar geometry. The most interesting aspect of the structures is that in both compounds the bite angle (P–Pt–P) is larger than that in the reported structure of dppfPtCl₂ and is in the order, dppfPtCl₂ (99.0°) [10] < dppfPtI₂ (100.6°) < dppfPtPh₂ (101.2°). The average Pt–P bond lengths of these compounds (dppfPtCl₂ = 2.260 Å, dppfPtI₂ = 2.283 Å, dppfPtPh₂ = 2.313 Å) also show similar trends. The relatively higher bite angle and bond distance of **1** and **2** could be due to the steric bulkiness of the phenyl and iodo substituents on the metal. The P···P distances in dppfPtI₂ and dppfPtPh₂, 3.510 and 3.574 Å, respectively, show the same trend, which is consistent with the above findings, although no data from the literature is available for comparison. Interestingly, the X–Pt–X (X = Cl [10], I) bond angles of dppfPtCl₂ and dppfPtI₂ are very close to each other, and are 85.8(2)° and 86.1(1)°, respectively. However, the analogous bond angle for C–Pt–C angle in dppfPtPh₂ is much smaller, 82.9(2)°.

In Pd chemistry, Hayashi et al. ([2]a), has made a comparative study on the catalytic activity of dppfPdCl₂ with that of the other bidentate phosphine complexes. The study correlated that compounds with larger P–Pd–P bond angles (bite angles) and smaller Cl–P–Cl bond angles have superior activity and selectivity in Grignard cross coupling reactions, as they can accelerate reductive elimination due to the presence of serious strain in the chelating system, which would be released by the dissociation of the phosphino group. For example, the reaction of *n*-butylmagnesium chloride with a series of bromobenzene derivatives, in pres-

Table 6
³¹P and ¹³C-NMR spectral data of dppf, dppfPtI₂ and dppfPtPh₂ in CDCl₃

Atom numbering	dppf δ (ppm)	dppfPtI ₂ δ (ppm)	dppfPtPh ₂ δ (ppm)
P	-16.6	10.1 (¹ J _{Pt-P} = 3551.8) (² J _{P-P'} = 7.0)	15.7 (¹ J _{Pt-P} = 1782.9) (² J _{P-P'} = 15.8)
C1	76.7 (¹ J _{P-C1} = 7.1)	74.4 (¹ J _{P-C1} = 62.2) (³ J _{P'-C1} = 3.4) ² J _{Pt-C1} = 34.6	[76.3] [(¹ J _{P-C1} = 46.4)] [(³ J _{P'-C1} = 2.4)] (² J _{Pt-C1} = 25.7)
C2	73.7 (² J _{P-C2} = 14.8)	75.6 (² J _{P-C2} + ⁴ J _{P'-C2} = 17.1) (³ J _{Pt-C2} = a)	74.5 (² J _{P-C2} + ⁴ J _{P'-C2} = 10.1) (³ J _{Pt-C2} = a)
C3	72.4 (³ J _{P-C3} = 3.3, 1.3)	73.5 (² J _{P-C3} + ⁵ J _{P'-C3} = 6.4)	72.5[73.0] (³ J _{P-C3} + ⁵ J _{P'-C3} = 5.8)
C4	138.9 (¹ J _{P-C4} = 9.6)	133.1 (¹ J _{P-C4} = 64.8) (³ J _{P'-C4} = 1.0) (² J _{Pt-C4} = 34.6)	133.8[134.0] (¹ J _{P-C4} = 48.4) (³ J _{P'-C4} = 1.6) (² J _{Pt-C4} = 24.4)
C5	133.4 (² J _{P-C5} = 19.6)	135.2 (² J _{P-C5} + ⁴ J _{P'-C5} = 10.7) (³ J _{Pt-C5} = a)	134.5 [134.8] (² J _{P-C5} + ⁴ J _{P'-C5} = 11.2) (³ J _{Pt-C5} = 16.7)
C6	128.1 (³ J _{P-C6} = 6.4)	127.7 (³ J _{P-C6} + ⁵ J _{P'-C6} = 11.7) (⁴ J _{Pt-C6} = \approx 0)	127.5 [127.9] (³ J _{P-C6} + ⁵ J _{P'-C6} = 9.8) (⁴ J _{Pt-C6} = \approx 0)
C7	128.4 (⁴ J _{P-C7} = \approx 0)	130.1 (⁴ J _{P-C7} = \approx 0)	129.1 [129.9] (⁴ J _{P-C7} = \approx 0)
C8	—	—	160.7 [161.7] (² J _{P-C8} = 11.5, <i>cis</i> ; 110.8, <i>trans</i>) (¹ J _{Pt-C8} = 848.2)
C9	—	—	136.2 [136.6] (³ J _{P-C9} <i>cis</i> + <i>trans</i> = b) (¹ J _{Pt-C9} = 29.4)
C10	—	—	126.9 [127.2] (⁴ J _{P-C10} 0 <i>cis</i> + <i>trans</i> = 5.8) (³ J _{Pt-C10} = 66.6)
C11	—	—	120.3 [120.7] (⁵ J _{P-C11} = \approx 0) (⁴ J _{Pt-C11} = 11.4)

Data in square brackets refer to the values in CD₂Cl₂ solvent. Coupling constants are absolute values in Hz, and are given in parenthesis.

^a Cannot report J_{Pt-C} due to the overlap of ¹⁹⁵Pt satellite lines 1 and 5 of AXX' pentuplet.

^b Line broadening obscures coupling, but less than 3 Hz.

ence of dppePdCl₂ and dpppPdCl₂ gave 0–4% and 4–75% yields of the coupled products respectively, while dppfPdCl₂ gave above 95% yield in most of the cases. This difference in reactivity is attributed to their respective P–Pd–P bond angles, 85.5°, 90.6° and 99.07° for dichloro[1,1'-bis(diphenylphosphino)ethane]palladium(II) [19], dichloro[1,1'-bis(diphenylphosphino)propane]palladium(II) [19] and dichloro[1,1'-bis(diphenylphosphino)ferrocene]palladium(II). Although we have not done any similar catalytic studies, the above data suggest that our compounds may be equally good or even superior, in related studies.

The phosphorus atoms in both these complexes are distorted from the ideal tetrahedral geometry. For example, the Pt–P–C(Cp) bond angles of **1** deviate from the ideal tetrahedral angle, 109.45°, to an average bond angle of 121°. In complex **2**, the two Pt–P–C(Cp) bond

angles are non identical, and are 121.4(5)° and 114.6(6)°, respectively for P(1) and P(2) centers.

3.1. NMR spectral study

¹H- and ¹³C-NMR chemical shifts with the coupling constants are given in Tables 5 and 6, respectively, for dppf, dppfPtI₂ and dppfPtPh₂ (Fig. 3). Proton and ¹³C shifts for dppf are available in the literature [20] with no listings of coupling constants.

The phenyl protons in dppf have close shift values and are reported as a range. This is similar to the pattern obtained for triphenylphosphine in CDCl₃. Coordination to Pt diverges all phenyl ring proton shift values. The *ortho* proton patterns become easy to identify by appearance. This allows absolute identification

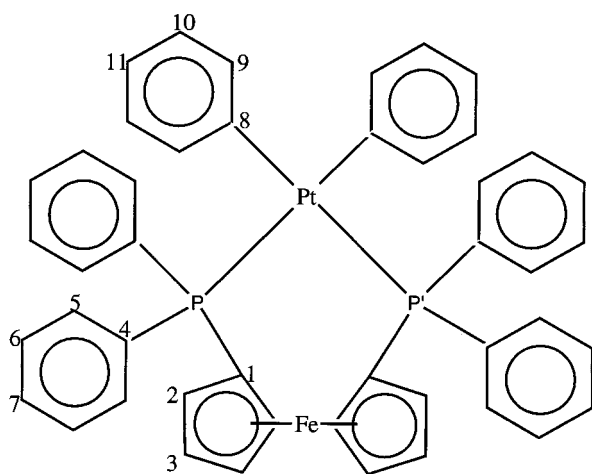


Fig. 3. Numbering scheme used to interpret the NMR spectra of dppf, dppfPtI₂ and dppfPtPh₂.

of all other phenyl protons. For the cyclopentadienyl ring, the assignment of the quartet in the free ligand to H-2 is based on the additional coupling coming from phosphorus. In the absence of this coupling, it is expected that H-2 and H-3 would be 'triplet like' from a high order AA'XX' system.

A low resolution HETCOR shows H-2 correlated with the cyclopentadienyl carbon with the larger phosphorus coupling, in analogy with C-5 and C-6 in the

phenyl ring of dppf. The quartet is used to distinguish H-2 from H-3 in dppfPtI₂ and dppfPtPh₂. ¹⁹⁵Pt satellites were found for H-9 in dppfPtPh₂, but no other protons appeared to have measurable Pt satellites. A HETCOR 2D-map shown in Fig. 4 is used to confirm all phenyl carbon assignments for dppfPtPh₂. These are used to confirm assignments in dppfPtI₂. Low resolution HETCOR is used to correlate cyclopentadienyl carbon shifts. C-2 and C-3 keep the same relative shift order in dppf, dppfPtI₂ and dppfPtPh₂, but H-2 and H-3 change shift positions in dppfPtPh₂. This may be due to a slight shielding effect at the cyclopentadienyl ring when phenyl rings are put on to the Pt atom. It should be noted that, except for C-8 shift, the carbon shifts and *J*_{Pt-C} couplings of the Pt-phenyls are quite similar to *trans*-PhPt(AsMe₂)₂Cl [21].

Most of the carbon resonances in dppf appear as simple doublets due to the couplings with the phosphorus atom. However C-3 has two couplings, the smaller one could be due to a long-range coupling through the ferrocene iron to the phosphorus atom. As reported in the literature, coordination to the Pt results in a high order pattern [22] due to the presence of a non-zero value for ²*J*_{P-P}. The high order patterns were simulated to extract the correct *J* values. The carbon-phosphorus couplings reported in Table 5 are as absolute values, although certain sign relationships are required to obtain the correct computer simulation for each multiplet.

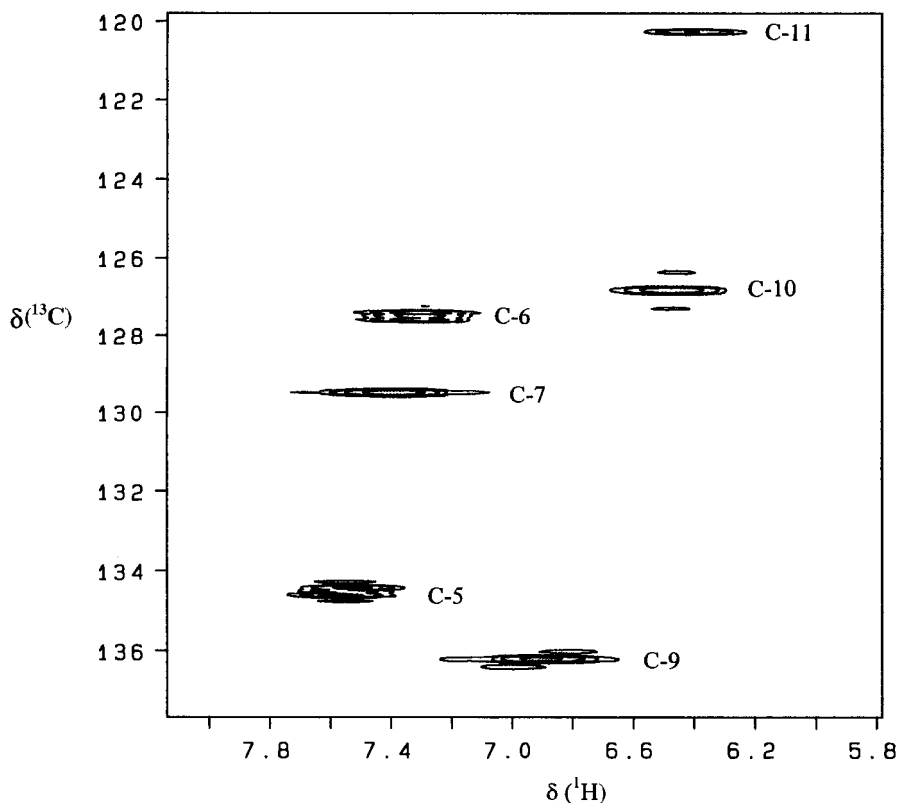


Fig. 4. A section of the 2D HETCOR map of dppfPtPh₂, showing the P-phenyl and Pt-phenyl region.

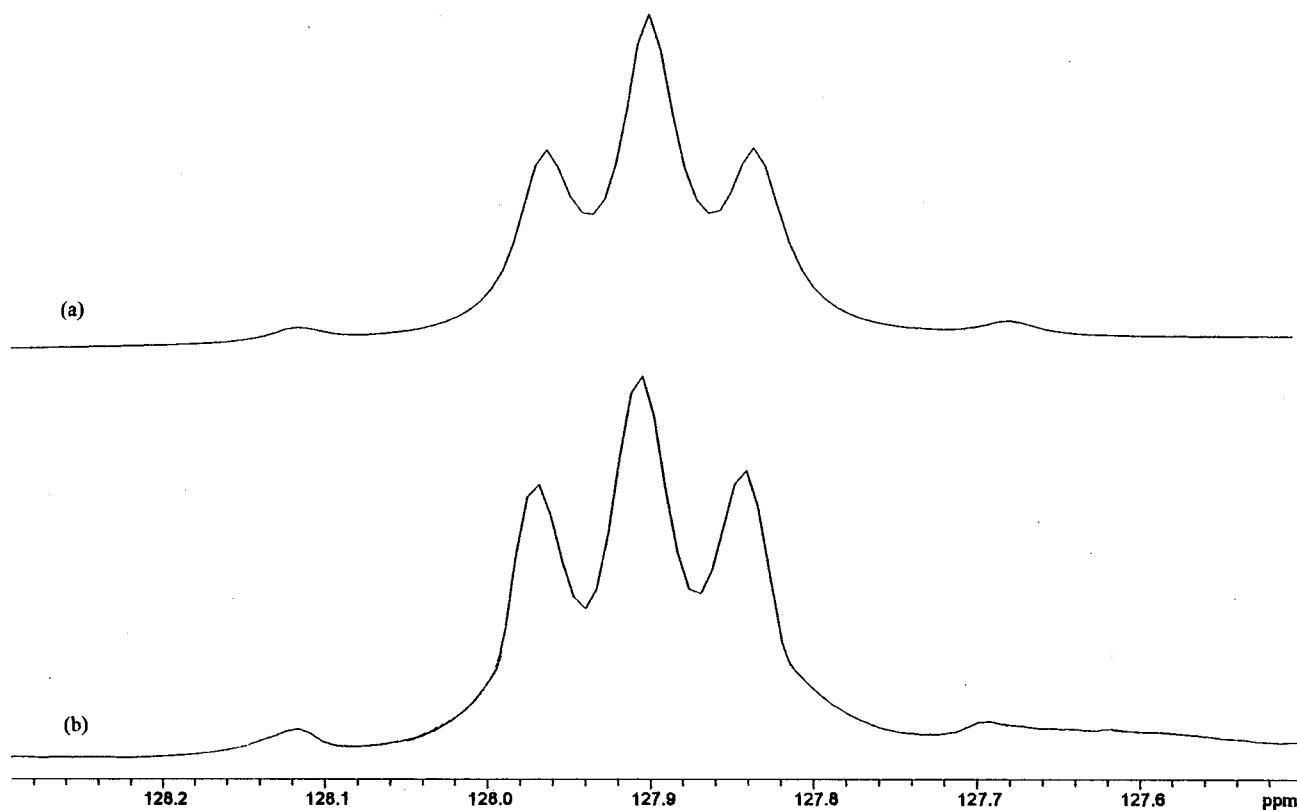


Fig. 5. Simulated (a) and experimental (b) spectrum of the C6 resonance of dppfPtI₂ (CD₂Cl₂, 75.5 MHz).

The major pattern in the carbon resonances for C-1, C-4 and C-8 in dppfPtI₂ and dppfPtPh₂ are a doublet of doublets, except for C-4 of dppfPtI₂, which is a doublet. All of these resonances also show a minor 1.5–2.0 Hz doublet in the center of the pattern. The absolute value of ${}^2J_{\text{P-P}}$ is required to simulate the multiplets at C-1, C-4 and C-8 in dppfPtI₂ and dppfPtPh₂, although either sign gives the correct simulation. Since the resonances for C-2, and C-5 in the Pt complexes were obscured by Pt satellites, and the lines in C-3 resonances were masked by noise, we could not determine the ${}^2J_{\text{P-P}}$ values from these multiplets. However, accurate determination of ${}^2J_{\text{P-P}}$ was achieved by using lines 1 and 5 in C-6 resonances. The relative sign of ${}^1J_{\text{P-C}}$ and ${}^3J_{\text{P-C}}$ must be of the same convention to get the correct simulation of C-1 and C-4 resonances in both complexes. The proper simulation of C-8 in dppfPtPh₂ requires that ${}^2J_{\text{P-C8 cis}}$ and ${}^2J_{\text{P-C8 trans}}$ couplings should be of opposite sign. This is similar to the case of a carbon–phosphorus coupling through Pt in *cis*-[PtMe₂(PMe₂Ph)₂] [23]. Values for $|{}^N J_{\text{P-C}} + {}^{N+2} J_{\text{P-C}}|$ among the remaining carbons are derived from the difference in lines 2 and 4 in pentuplets of C-2, C-3, C-5, C-6, and C-10 in dppfPtI₂ and dppfPtPh₂. An example of the pentuplet pattern for the experimental and simu-

lated C6 resonances in the ¹³C spectrum of dppfPtPh₂ is given in Fig. 5.

The ³¹P-NMR shifts are listed in Table 6. The chemical shift for dppfPtI₂ (10.1 ppm) is similar to that in the chloro analog, dppfPtCl₂ (13.6 ppm) [10]. Replacement of iodine by Ph in dppfPtPh₂ shifts the value to 15.7 ppm. A previously reported value (124.14 ppm) [10] for the ligand, dppf, seems to be an error. Our shifts for dppf (–16.6 ppm) is same as the reported value, –16.6 ppm [20]. The Pt–P coupling constants present no surprises. The ${}^1J_{\text{Pt-P}}$ coupling in dppfPtI₂ (3551.8 Hz) is very close to that in the chloro analog [10]. A decreased ${}^1J_{\text{Pt-P}}$ value (1782.9 Hz) in dppfPtPh₂ reflects the well known *trans* influence [24] of an aryl or alkyl group.

3.2. Summary

Two potential Pt based homogenous catalysts were synthesized in nearly quantitative yield with excellent purity and were characterized unambiguously. The activities of these complexes are being tested elsewhere. The synthesis of Pd–alkyl based complexes are currently in progress in our laboratory, mainly to investigate their potential applications in organic synthesis and also in polymer synthesis using homogeneous catalysis.

4. Supporting information available

Observed and calculated structure factors, complete list of bond angles and bond lengths, and final atomic coordinates with anisotropic displacement coefficients are deposited. Ordering information is given on any current masthead page.

Acknowledgements

Acknowledgments are due to Dr William H. Tamblin, Technical Director, Chemicals and Catalysts Development, Precious Metals Division, Johnson Matthey, West Deptford, New Jersey for the encouragement in this work. Dr Ernest S. Gore of the same department is also thanked for the useful discussion.

References

- [1] (a) K.-S. Gan, T.S.A. Hor, in: A. Togni, T. Hayashi (Eds.), *Ferrocenes*, VCH, Weinheim, 1995. (b) W.R. Cullen, J.D. Woolins, *Coord. Chem. Rev.* 39 (1982) 1. (c) T. Hayashi, M. Kumada, *Acc. Chem. Res.* 15 (1982) 395.
- [2] (a) T. Hayashi, M. Konishi, Y. Kabori, M. Kumada, T. Higuchi, K. Hirotsu, *J. Am. Chem. Soc.* 106 (1984) 158 (see references therein). (b) T. Hayashi, M. Konishi, H. Ito, M. Kumada, *J. Am. Chem. Soc.* 104 (1982) 4962. (c) M. Kumada, *Pure Appl. Chem.* 52 (1980) 669. (d) J.M. Brown, N.A. Cooley, *Organometallics* 9 (1990) 353. (e) T. Hayashi, M. Konishi, M. Fukushima, T. Mise, M. Tajika, M. Kumada, *J. Am. Chem. Soc.* 104 (1982) 189. (f) F. Diederich, P.J. Stang (Eds.), *Metal-catalyzed Cross-coupling Reactions*, Wiley-VCH, Weinheim, 1998.
- [3] (a) W.R. Cullen, T.D. Appleton, S.V. Evens, T.J. Kim, J.T. Trotter, *J. Organomet. Chem.* 279 (1985) 5. (b) I.R. Butler, W.R. Cullen, T.-J. Kim, S.J. Rettig, J. Trotter, *Organometallics* 4 (1985) 972. (c) W.R. Cullen, F.W.B. Einstein, T. Jones, T.-J. Kim, *Organometallics* 2 (1983) 714. (d) W.R. Cullen, J.D. Woolins, *Can. J. Chem.* 60 (1982) 1793. (e) T.-J. Kim, K.-C. Lee, *Bull. Korean Chem. Soc.* 10 (1989) 279.
- [4] (a) T. Hayashi, M. Konishi, K.-I. Yokota, M. Kumada, *J. Organomet. Chem.* 285 (1985) 359. (b) T. Hayashi, M. Konishi, K.-I. Yokota, M. Kumada, *J. Chem. Soc. Chem. Commun.* (1981) 313.
- [5] (a) W.R. Cullen, T.J. Kim, F.W.B. Einstein, T. Jones, *Organometallics* 4 (1985) 316. (b) P.L. Castle, D.A. Widdowson, *Tetrahedron Lett.* 27 (1986) 6013. (c) K. Yunan, W.J. Scott, *J. Org. Chem.* 55 (1990) 6188.
- [6] (a) O.R. Hughes, J.D. Unruh, *J. Mol. Catal.* 12 (1981) 71. (b) O.R. Hughes, D.A. Young, *J. Am. Chem. Soc.* 103 (1981) 6636.
- [7] (a) B.M. Trost, T.S. Scanlan, *J. Am. Chem. Soc.* 111 (1989) 4988. (b) Y. Ito, M. Sawamura, M. Matsuoka, Y. Matsumoto, T. Hayashi, *Tetrahedron Lett.* 28 (1987) 4849.
- [8] (a) T. Kobayashi, M. Tauaka, *J. Chem. Soc. Chem. Commun.* (1981) 333. (b) V.N. Kalinin, M.V. Shostakovskiy, A.B. Ponomaryov, *Tetrahedron Lett.* 33 (1992) 373. (c) K. Itoh, M. Miura, M. Nomura, *Tetrahedron Lett.* 33 (1992) 5369.
- [9] (a) R. Galarini, A. Musco, R. Pontellini, A. Bolognesi, S. Destri, M. Catellani, M.; Mascherpa, G. Zhuo, *J. Chem. Soc. Chem. Commun.* (1991) 364. (b) E. Crammer, V. Percec, *J. Polymer Sci.; Part A: Polymer Chem.* 28 (1990) 3029.
- [10] G.M. De Lima, C.A.L. Filguerias, *Trans. Met. Chem.* 20 (1995) 380.
- [11] R.D. Kelly, G.B. Young, *Polyhedron* 8 (1989) 433.
- [12] P. Stang, K. Olenyuk, J. Fan, A. M. Arif, *Organometallics* 15 (1996) 904.
- [13] (a) C. M. Killan, D. J. Tempel, L. K. Johnson, M. Brookhart, *J. Am. Chem. Soc.* 118 (1996) 11664. (b) F.C. Rix, M. Brookhart, P.S. White, *J. Am. Chem. Soc.* 118 (1996) 4746. (c) L.K. Johnson, S. Mecking, M. Brookhart, *J. Am. Chem. Soc.* 118 (1996) 267. (d) L.K. Johnson, C.M. Killian, M. Brookhart, *J. Am. Chem. Soc.* 117 (1995) 6414. (e) F.C. Rix, M. Brookhart, *J. Am. Chem. Soc.* 117 (1995) 1137. (f) M. Brookhart, F.C. Rix, J.C. DeSimone, J.C. Barborak, *J. Am. Chem. Soc.* 114 (1992) 5895. (g) J. Feldman, S.J. McLain, A. Parthasarathy, W.J. Marshall, J.C. Calabrese, S.D. Arther, *Organometallics* 16 (1997) 1514.
- [14] (a) G.S. Hill, L. Manojlovic-Muir, K.W. Muir, R.J. Puddephatt, *Organometallics* 16 (1997) 525. (b) L.M. Rendina, R.J. Puddephatt, *Chem. Rev.* 97 (1997) 1735.
- [15] D.D. Perrin, W.L.F. Armarego, *Purification of Laboratory Chemicals*, Pergamon Press, Oxford, UK, 1988.
- [16] A. Altomare, G. Cascarano, C. Giacovazzo, A. Guagliardi, M.C. Burla, G. Polidori, M. Camalli, *J. Appl. Cryst.* 27 (1994) 435.
- [17] G M. Sheldrick, *SHELXTL/PC User's Manual*, Siemens Analytical Instruments, Madison, Wisconsin, USA
- [18] T.J. Colacot, Private Communications, Johnson Matthey, West Deptford, NJ, 1996.
- [19] W.L. Steffin, G.J. Palenick, *Inorg. Chem.* 15 (1976) 2432.
- [20] R.-J. De Lang, J. Van Soolingen, H.R. Verkruijse, L. Brandsma, *Syn. Comm.* 25 (1995) 2989.
- [21] H.C. Clark, J.E.H. Ward, *J. Am. Chem. Soc.* 96 (1974) 1741.
- [22] (a) R.J. Abraham, H.J. Berstein, *Can. J. Chem.* 39 (1961) 216. (b) D.A. Redfield, L.W. Cary, H.J. Nelson, *Inorg. Chem.*, 14 (1975) 50.
- [23] A.J. Cheney, B.E. Mann, B.L. Shaw, *J. Chem. Soc. Chem. Commun.* (1979) 431.
- [24] (a) F.H. Allen, A. Pidcock, *J. Chem. Soc. (A)* (1968) 2700. (b) F.H. Allen, S.N. Sze, *J. Chem. Soc. (A)* (1971) 2054.